

Identification of the PIP₂-binding site on Kir6.2 by molecular modelling and functional analysis

Shozeb Haider^{1,3,4}, Andrei I Tarasov^{2,3},
Tim J Craig², Mark SP Sansom¹
and Frances M Ashcroft^{2,*}

¹Department of Biochemistry, University of Oxford, Oxford, UK
and ²Laboratory of Physiology, University of Oxford, Oxford, UK

ATP-sensitive potassium (K_{ATP}) channels couple cell metabolism to electrical activity by regulating K⁺ fluxes across the plasma membrane. Channel closure is facilitated by ATP, which binds to the pore-forming subunit (Kir6.2). Conversely, channel opening is potentiated by phosphoinositol bisphosphate (PIP₂), which binds to Kir6.2 and reduces channel inhibition by ATP. Here, we use homology modelling and ligand docking to identify the PIP₂-binding site on Kir6.2. The model is consistent with a large amount of functional data and was further tested by mutagenesis. The fatty acyl tails of PIP₂ lie within the membrane and the head group extends downwards to interact with residues in the N terminus (K39, N41, R54), transmembrane domains (K67) and C terminus (R176, R177, E179, R301) of Kir6.2. Our model suggests how PIP₂ increases channel opening and decreases ATP binding and channel inhibition. It is likely to be applicable to the PIP₂-binding site of other Kir channels, as the residues identified are conserved and influence PIP₂ sensitivity in other Kir channel family members.

The EMBO Journal (2007) 26, 3749–3759. doi:10.1038/sj.emboj.7601809; Published online 2 August 2007

Subject Categories: membranes & transport; molecular biology of disease

Keywords: diabetes; hyperinsulinism; K_{ATP} channel; molecular dynamics; PIP₂-binding site

Introduction

Anionic phospholipids, such as phosphoinositol bisphosphate (PIP₂) and phosphoinositol trisphosphate (PIP₃), interact with members of the inwardly rectifying family of potassium channels (Kir channels). In eukaryotic Kir channels, this results in channel activation (Fan and Makielski, 1997; Baukrowitz *et al*, 1998; Shyng and Nichols, 1998), whereas in the bacterial channel KirBac1.1 it causes channel inhibition (Enkvetchakul *et al*, 2005). The pore-forming

subunit of the ATP-sensitive potassium (K_{ATP}) channel belongs to the Kir family (Sakura *et al*, 1995), and inositol phospholipids are found to have multiple effects on K_{ATP} channels. Thus, PIP₂ increases the channel open probability (*P*_o) by prolonging the open time and shortening the closed times (Fan and Makielski, 1999). It also reduces the channel sensitivity to inhibition by ATP (Fan and Makielski, 1997, 1999; Baukrowitz *et al*, 1998; Shyng and Nichols, 1998). This appears to involve two effects. First, PIP₂ has been shown to directly decrease the binding of ATP analogues to purified Kir6.2 (Wang *et al*, 2002) or to the C terminus of Kir6.2 (MacGregor *et al*, 2002). Secondly, the increase in open probability produced by PIP₂ will (indirectly) reduce the channel ATP sensitivity (Trapp *et al*, 1998; Enkvetchakul *et al*, 2000). PIP₂ also decreases K_{ATP} channel activation by MgADP, reduces channel inhibition by sulphonylureas (Krauter *et al*, 2001) and attenuates rundown (Fan and Makielski, 1997); all these effects, however, are likely to be a consequence of the change in *P*_o. The effects on *P*_o and ATP sensitivity appear to be distinct, as they can be separated temporally (Fan and Makielski, 1999).

K_{ATP} channels are octamers of Kir6.2x and SUR subunits (for review, see Haider *et al*, 2005a). Four inwardly rectifying subunits (Kir6.2 or Kir6.1) form the channel pore. Each is associated with a regulatory sulphonylurea receptor subunit (SUR1 or SUR2). Although neither subunit trafficks to the surface membrane in the absence of its partner, a truncated form of Kir6.2 (Kir6.2ΔC) is able to reach the membrane (Tucker *et al*, 1997) and can be used to study the effects of phosphoinositides on Kir6.2 in the absence of SUR. Such studies have shown that phosphoinositides can activate Kir6.2ΔC, albeit not as potently as when SUR is present (Baukrowitz *et al*, 1998). Furthermore, the effects of phosphoinositides are similar for Kir6.2/SUR1 and Kir6.2/SUR2 channels (Fan and Makielski, 1999; Baukrowitz *et al*, 1998; Shyng and Nichols, 1998). Thus, the phosphoinositide-binding site must lie on the Kir6.2 subunit. In confirmation of this idea, PIP₂ has been shown to bind directly to purified recombinant Kir6.2 (Wang *et al*, 2002).

To understand how PIP₂ activates the K_{ATP} channel and how mutations in Kir6.2 impair this process, it is necessary to identify the location and structure of the PIP₂-binding site. The structure of this site is unknown, but many experiments suggest that it involves residues from both the N- and C-terminal domains of Kir6.2 (Fan and Makielski, 1997; Shyng *et al*, 2000; Cukras *et al*, 2002; MacGregor *et al*, 2002; Schulze *et al*, 2003).

Attempts to crystallise Kir6.2, or its C-terminal domains, have proved unsuccessful. However, the crystal structures of a putative bacterial Kir channel, KirBac1.1 (Kuo *et al*, 2003) and of the N- and C-terminal domains of its eukaryotic counterparts Kir3.1 and Kir2.1 (Nishida and MacKinnon, 2002; Pegan *et al*, 2005), have been solved. We previously used these structures to construct a molecular model of the Kir6.2 tetramer, and employed ligand docking to identify

*Corresponding author. Department of Physiology, Anatomy and Genetics, University of Oxford, Parks Road, Oxford OX1 3PT, UK.
Tel.: +44 1865 285810; Fax: +44 1865 285811;
E-mail: fma@dpag.ox.ac.uk

³These authors contributed equally to this work

⁴Present address: The London School of Pharmacy, 29–39 Brunswick Square, London WC1N 1AX, UK

Received: 16 January 2007; accepted: 3 July 2007; published online: 2 August 2007

residues interacting with ATP (Antcliff *et al*, 2005; Haider *et al*, 2005a). The model we proposed is consistent with a large amount of functional data and was further validated by additional site-directed mutagenesis (Antcliff *et al*, 2005). Subsequently, over 20 different Kir6.2 mutations that cause neonatal diabetes in humans have been identified and shown to decrease the channel ATP sensitivity (Ashcroft, 2005). In most cases, the model was able to satisfactorily explain the functional effects of the mutations, as these were found to lie within the putative ATP-binding site, or in regions of the channel associated with gating, such as the slide helix and gating loops.

In this paper, we use the same model for Kir6.2 (Antcliff *et al*, 2005) and employ ligand docking and molecular dynamics simulations to identify the binding site for PIP₂. Our results suggest the location and structure of the four PIP₂-binding sites. They further show that, although ATP and PIP₂ do not share the same binding site, some residues may contribute to both sites. Finally, our results provide some suggestions for how PIP₂ binding may lead to an increase in K_{ATP} channel open probability and a reduction in ATP sensitivity.

Results

Molecular modelling and ligand docking

A homology model of the mouse Kir6.2 (residues 32–358; GenBank D50581) tetramer was constructed based on the X-ray crystal structures of KirBac1.1 (PDB id 1P7B) (Kuo *et al*, 2003) and the intracellular (IC) domains of rat Kir3.1 (PDB id 1N9P) (Nishida and MacKinnon, 2002). This has been described in detail previously, and was successfully used to identify the ATP-binding site on Kir6.2 (Antcliff *et al*, 2005; Haider *et al*, 2005a). We now use this model to aid identification of residues contributing to the binding site for PI(4,5)P₂, here abbreviated as PIP₂.

The PIP₂-binding site was identified using automated ligand docking. The PIP₂ molecule consists of a long hydrophobic acyl tail and a negatively charged inositol trisphosphate head group. Simulations of the PIP₂ molecule within a POPC bilayer reveal that it can extend up to ~17 Å beyond the inner leaflet of the membrane and that the IP₃ head group is flexible and may adopt several different conformations (for example, it can sit both parallel to, and perpendicular to, the membrane) (Sansom *et al*, 2005).

Electrostatic potential surface maps of the Kir6.2 model reveal a band of positive charge located close to the inner leaflet of the membrane (Figure 1A). This region is sufficiently close to the membrane to be accessible to the negatively charged head group of PIP₂ when the lipid tails lie within the bilayer. A grid encompassing all of these positively charged residues was placed around this region (Figure 1A) and used in docking calculations to search for putative binding sites for the PIP₂ head group, *D*-myo-IP₃ (IP₃). IP₃, rather than PIP₂, was used in the docking studies, because the flexibility and hydrophobicity of the acyl chains of PIP₂ could impair the docking procedure. Ranking the IP₃-protein interaction energies from 200 docks revealed two distinct binding sites on each subunit of the Kir6.2 model (Figure 1B). The presence of discrete docking clusters is encouraging, as this is indicative of a 'good' homology model (Holyoake *et al*, 2006).

Of the two possible sites, one was situated within the cytosolic pore (site b in Figure 1B) and was rejected, as it was unable to accommodate the acyl tails of the intact PIP₂ molecule. The other site was therefore assumed to be the physiological binding site (site a in Figure 1B). For this site, the 50 docks with the most favourable interaction energies were filtered to identify the preferred binding mode (Figure 1C). The final conformation of the docked IP₃ head group was selected on the basis of the ability of bound PIP₂ to interact with the lipid bilayer. Thus, the orientation of the docked ligand had to be such that the acyl tails attached to the IP₃ head group could be extended into the membrane and the maximum distance between the IP₃ head group and the membrane had to be less than ~17 Å (Sansom *et al*, 2005). The docking site was identified based on these criteria and a favourable ligand-protein interaction energy. A diacyl glycerol (1-palmitoyl-2-arachidonyl-glycerol) was then added to the IP₃ head group of PIP₂. The conformation of the tail was taken from a separate simulation in which the PIP₂ molecule alone was simulated in a POPC bilayer (Sansom *et al*, 2005). The Kir6.2 model with bound PIP₂ was then subjected to energy minimisation to relieve any steric clashes that might have arisen between the protein side chains and PIP₂.

It is likely that the crystal structures of both KirBac1.1 and Kir3.1 represent closed states of the channels. First, KirBac1.1 is clearly closed, as bulky side-chain residues occlude access of hydrated K⁺ to the cytosolic mouth of the pore (Kuo *et al*, 2003). Second, Kir3.1 is activated by binding Gβγ proteins, and the IC domains were crystallised in the absence of ligand (Nishida and MacKinnon, 2002). Thus, we assume that these structures form a reasonable template for the closed state of Kir6.2, in which ATP is bound. Therefore, one might argue that the structure would not be adequate to describe the open state, in which PIP₂ is bound. However, this caveat may not apply to models based on KirBac1.1, which is in fact inhibited by PIP₂ (Enkvetchakul *et al*, 2005). We therefore argue that the binding site for phosphoinositides may be the same in KirBac and Kir channels, and that whether channel is opened or closed by these ligands depends on other factors/residues, which influence how binding is coupled to gating.

The K_{ATP} channel comprises both Kir6.2 and SUR subunits and it is possible that SUR imposes conformational constraints on Kir6.2. Our model corresponds most closely to Kir6.2ΔC, a truncated form of Kir6.2 that expresses in the absence of SUR1 (Tucker *et al*, 1997). However, literature on the effects on PIP₂ on Kir6.2ΔC (as compared to Kir6.2/SUR1) is scarce. Thus, in our discussions below, functional data are quoted for Kir6.2/SUR1, unless it is specifically stated that they were measured for Kir6.2ΔC.

Simulations

To explore the interactions of PIP₂ with the Kir6.2 channel protein, and the conformational dynamics of the protein model, four simulations (see Table I) were performed: with/without PIP₂ and with/without ATP at their respective binding sites. The conformational stability of the Kir6.2 model in the four simulations was assessed by carrying out a 10-ns molecular dynamics simulation of each model in a lipid (POPC) bilayer. Previous experience suggests that a 10-ns simulation is sufficient to reveal any major conformational instability within the model (Capener *et al*, 2000). Thus, a simple measure of the 'quality' of a model can be obtained by

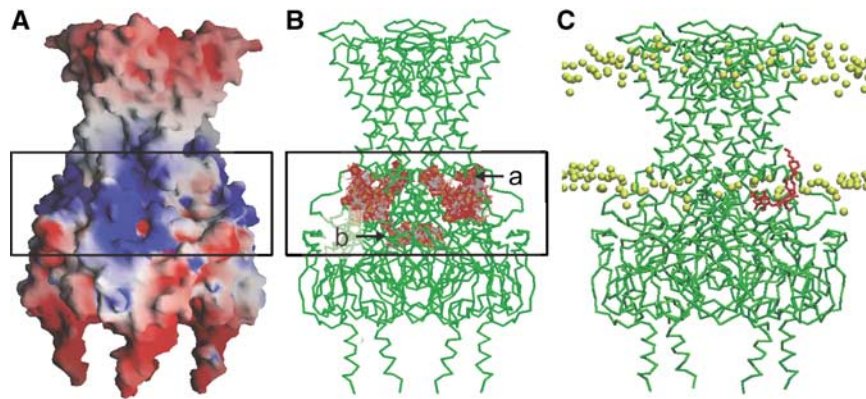


Figure 1 Models of the Kir6.2 tetramer viewed from side. (A) Surface electrostatic map of Kir6.2 model. The red colour corresponds to negatively charged regions and the blue colour to positively charged regions. The box placed over the central positively charged region defines the boundary within which the PIP₂ head group was allowed to dock. (B) Kir6.2 model (green) with the docked PIP₂ head group (IP₃, orange) as identified by the AUTODOCK programme. The grid defines the boundary within which the PIP₂ head group was allowed to dock. Two binding sites were observed (a) and (b): the lower one (b) was deemed not to be physiological (see text). (C) Kir6.2 model (green) placed in a POPC bilayer (the small yellow spheres represent phosphorus atoms) with one docked PIP₂ (red) positioned in its binding site. The acyl tails of PIP₂ extend to anchor it in the lipid bilayer.

Table I Summary of Simulations

Simulations	Ligands	C α RMSD (Å)	
		All residues	Core residues
Sim1	4 PIP ₂	4.1	3.5
Sim2	4 ATP	3.3	3.1
Sim3	4 ATP + 4 PIP ₂	3.2	3.1
Sim4	None	3.6	3.3

The C α RMSDs are relative to the initial structure and averaged over the final 2 ns of each simulation.

measuring the root mean square deviation (RMSD) of C α atoms from their position in the initial model as a function of time (Table I and Figure 4).

The degree of conformational drift revealed by the RMSD values is comparable to that seen in simulations of cryoelectron microscopy structures (resolution 3.5 Å) or in homology models of other Kir channels (Haider *et al*, 2005b), but is a little higher than that seen in simulations of high-resolution (2.2 Å or better) X-ray structures of membrane proteins (Law *et al*, 2005). If one restricts the C α RMSD calculation to the core regions of the transmembrane and IC domains (i.e., excluding the surface loops) the values are lower (Table I), indicating relatively small drifts in the Kir6.2 core. However, comparison of the core region C α RMSDs (Table I) for the four simulations suggests that, with respect to conformational drift on a 10-ns timescale, Sim2 (4 ATP) and Sim3 (4 ATP + 4 PIP₂) were a little more stable than Sim4 (no ligands), and that Sim1 (4 PIP₂) was the least stable.

The magnitude of the fluctuations of each individual residue can be used to define more mobile regions within the Kir6.2 model. In all four simulations, the maximal fluctuations were observed in residues 225–230 (which appear to be involved in intersubunit interactions) and residues 240–250 (which line the lower part of the conduction pathway in the IC domain). Similar residues show high mobility in simulations of homology models of other Kir channels (Haider *et al*, 2005b).

The PIP₂-binding site

There are four PIP₂-binding pockets, one per subunit, which extend from the IC face of the membrane to the membrane proximal region of the IC domain. The IP₃ head group sits about 16 Å from the membrane headgroup region and the lipid tails extend into the membrane (Figure 1C). The lipid chains are positioned roughly mid-way along the slide helix and extend to meet the outer transmembrane helix (TM1) around isoleucine 74. Residues at the inner end of the slide helix, for example, T62 and L66, also lie close to the lipid chains of PIP₂. However, this proximity does not imply these residues contribute a specific lipid-binding site, because the lipid tail is highly mobile.

Eight charged or polar side chains lie within 4.5 Å of the head group of PIP₂ in our model: K39 and N41 in the N-domain; K67 at the cytosolic end of TM1; and R176, R177, E179, Q299 and R301 in the C-domain of the same subunit (Figure 2). Like the ATP-binding site (Antcliff *et al*, 2005), the binding site for PIP₂ lies at the interface between two subunits. Most residues derive from a single subunit but R54, at the inner end of the neighbouring slide helix, also lies within 4.5 Å of PIP₂.

The head group of PIP₂ carries two phosphate groups at positions 4 and 5 on the inositol ring. We refer to these as P4 and P5. A third phosphate group, which we term P1, links the inositol ring to the glycerol. In our model, P1 forms a potential hydrogen bond with the side chain of N41, whereas P4 interacts electrostatically with the side chains of K39 and R54, and P5 interacts with R176 and R301.

To further test the model and the predicted PIP₂-binding site, we made three additional models, each containing a different mutation predicted to alter PIP₂ binding (R54E, K67L, R176A). We then attempted to dock PIP₂ using the same protocol. We observed that IP₃ did not interact with any of the mutant models, that is, the lipid did not dock into the binding site found for the wild-type channel. This is consistent with a role for R54E, K67L and R176A in PIP₂ binding.

We also attempted docking of PI(3,4)P₂ and PI(3,4,5)P₂ using the same protocol as for PI(4,5)P₂. Of the PI(3,4,5)P₂ docks, 66% had positive interaction energies indicating this

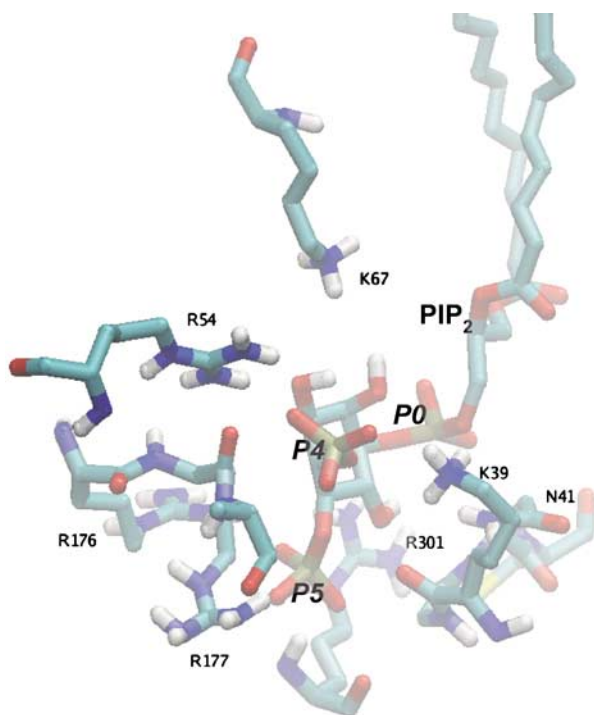


Figure 2 Model of PIP₂-binding pocket of Kir6.2 highlighting the charged and polar residues that lie close to PIP₂. All residues lie on the same subunit except for R54.

conformation is highly unfavourable. None of the remaining docks (44%) bound ligand in a conformation in which the acyl tails could be extended to the lipid membrane. Thus, PI(3,4,5)P₂ does not bind to our model. Some conformations of PI(3,4)P₂ bound in the PI(4,5)P₂-binding site, but their energies were much higher than that of PI(4,5)P₂. Furthermore, only 12% were in an orientation in which acyl tails could be extended into the membrane, compared with 35% for PI(4,5)P₂. This suggests that PI(3,4)P₂ binds poorly. However, there were two instances out of 200 in which PI(3,4)P₂ docked in almost exactly the same site as that of PI(4,5)P₂, and the interaction energies were within a comparable range.

Relationship of the PIP₂-binding site to the ATP-binding site

The ATP-binding site is distinct from that of the PIP₂-binding site. Nevertheless, the two sites lie adjacent to each other, the side chains of a β -strand (298–302; equivalent to the β -H strand in Kir3.1), separating the ligands such that PIP₂ binds towards the interior to the channel and ATP on its outer surface (Figure 3). They also share some of the same residues. In particular, K39, E179 and R301 contribute to both sites. Thus, the backbone of R301 interacts with the adenine ring of ATP, whereas the side chain of R301 lines the PIP₂-binding pocket and interacts with PIP₂-P5. Likewise, E179 interacts with both with PIP₂-P4 and with ATP. Neither of these residues has previously been reported to interact with PIP₂. However, some mutations at E179 alter the intrinsic gating of Kir6.2 (Antcliff *et al*, 2005), which is consistent with an interaction with PIP₂. Finally, the side chain of K39 interacts with PIP₂-P4, whereas the backbone lines the ATP-binding pocket. The model thus predicts that the adenine ring

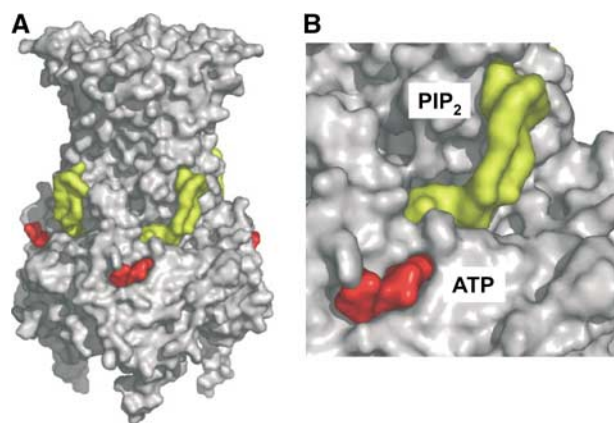


Figure 3 (A) Surface representation of the complete Kir6.2 model with docked ATP (red) and PIP₂ (yellow) molecules in their respective binding sites. (B) Close-up of a single binding site with surface representations of ATP and PIP₂.

of ATP lies within 3–4 Å of the phosphate groups on the head of PIP₂. This may explain why PIP₂ is able to displace ATP binding to Kir6.2 (Wang *et al*, 2002).

Further insight into ATP–PIP₂ interactions is provided by the simulations (Figure 4B). As previously reported (Antcliff *et al*, 2005), the phosphate tail of ATP makes three prominent interactions with Kir6.2: the α -phosphate with R201, the β -phosphate with K185 and the γ -phosphate with R50. All simulations show that the K185/ATP β P is the most persistent interaction and R201–ATP α P is the next most persistent. When ATP is present, but PIP₂ is absent (Sim2), both these interactions are maintained over the entire 10-ns simulation time. In contrast, the R50–ATP γ P interaction is intermittent, due to the fact that R50 lies on a loop contributed by the adjacent subunit. Thus, R50 appears to serve as a ‘gate’ for the ATP-binding site. Indeed, R50 is likely to move to enable ATP to enter its binding site, which may explain why it was necessary to remove the N terminus to dock ATP (Antcliff *et al*, 2005).

When PIP₂ (but not ATP) is present (Sim1), the net negative charges on the IP₃ head group are stabilised by several positively charged residues in Kir6.2, as described above. Of interest is that R50, which lies in a flexible loop (Figure 5A), is pulled towards the PIP₂-binding site and finally stabilised in this position, leaving the entrance to the ATP-binding site open (Figure 5B). When both PIP₂ and ATP are present at the start of the simulation, the interaction with PIP₂ proves to be dominant. Early (<2 ns) during the simulation, the R50–ATP γ P interaction is broken (>10 Å), and as a result, the gate to the ATP-binding site is partially opened. The R201–ATP α P interaction is the next to break (>6 Å), leaving only the K185–ATP β P interaction holding ATP in position. Fluctuations in the PIP₂-binding site eventually result in breaking of the K185–ATP β P bond.

Functional studies

The model accounts for a large amount of published data on PIP₂–K_{ATP} channel interactions (see Discussion). This provides significant validation of the model, as none of this information was used in its construction. In addition, we made new mutations to test the predictive power of the model.

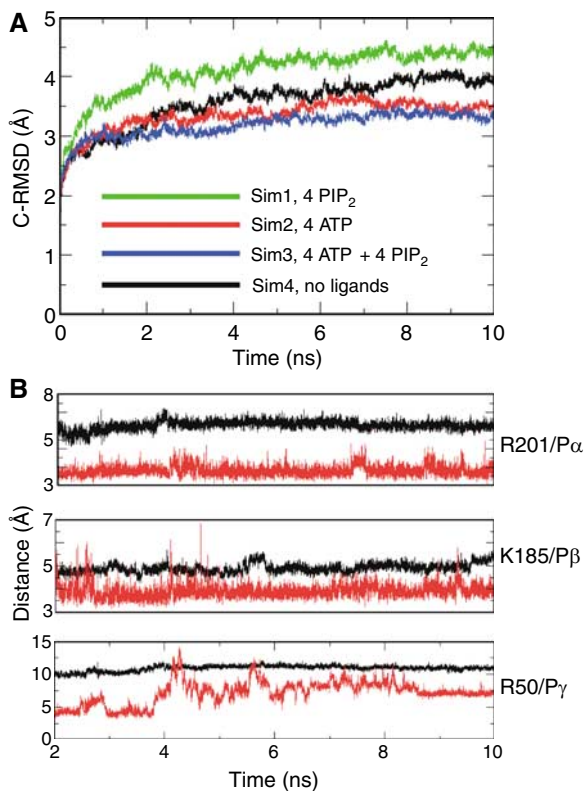


Figure 4 (A) C α -RMSDs (for all residues) from the initial structure plotted versus time for the different simulations: Sim1, Kir6.2 + 4 PIP₂ (green); Sim2, Kir6.2 + 4 ATP (red); p Sim3, Kir6.2 + 4 ATP + 4 PIP₂ (blue); Sim4, Kir6.2 (black). (B) Minimum distance between R201 α -phosphate (top), K185 β -phosphate (middle) and R50 γ -phosphate (bottom) compared between two different simulations, when ATP was present alone (Sim2, red) and when ATP was simultaneously present in its binding site along with PIP₂ (Sim1, black). R201-ATP and K185-ATP interactions are maintained throughout the simulation in model 2, but the R50-ATP γ P interaction is broken midway during the simulation. In model 3, the interaction is broken early in the simulation.

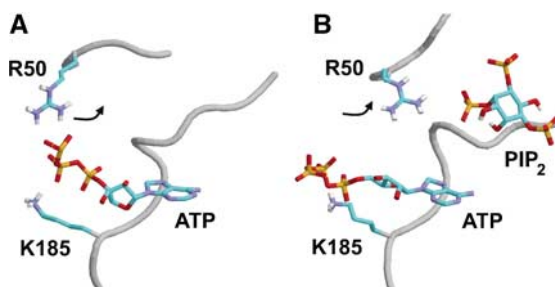


Figure 5 Position of R50 in Sim2 (A) and in Sim3 (B). In Sim2, the R50-ATP γ P interaction is maintained. However, in the presence of PIP₂ (Sim3), the R50-ATP γ P interaction is broken and R50 is pulled towards 4P in the PIP₂ head group.

The negative changes on the anionic head of PIP₂ are critical for activation of K_{ATP} channels. Phospholipids with less negative charge, such as PI, are significantly less effective at opening the channel (Fan and Makielski, 1997). Furthermore, polyvalent cations which complex PIP₂, such as neomycin and polylysine, reduce the functional effects of the lipid (Schulze *et al*, 2003). It is presumed that they do so by screening the negative charges on the PIP₂ headgroup, and

thereby reducing the effective concentration of PIP₂ in the membrane. Consequently, PIP₂ binding to the K_{ATP} channel is markedly decreased. Washout of neomycin restores the PIP₂ concentration, enabling it to interact with Kir6.2. Neomycin has previously been used to measure the PIP₂ sensitivity of K_{ATP} channels, with an increase in neomycin sensitivity being indicative of a decrease in PIP₂ binding (Schulze *et al*, 2003).

Half-maximal inhibition (IC₅₀) of Kir6.2/SUR1 was produced by 26 μ M neomycin (Figure 6A and Table II). This is similar to that reported for K_{ATP} channels in native beta-cells (20 μ M; Fan and Makielski, 1997). It is also close to that found for Kir6.2/SUR2A channels (17 μ M; Schulze *et al*, 2003), suggesting that the SUR subtype does not influence PIP₂ binding.

We tested the effect of mutating residues predicted to contribute to the PIP₂-binding site. As previously reported (Schulze *et al*, 2003), mutation of residues R54, K67 and R176 produced much smaller currents than wild type. The IC₅₀ for neomycin inhibition of Kir6.2/SUR1 was also reduced to 6 μ M for R54E and R54L, 2 μ M for R176A and 0.7 μ M for K67L (Figure 3A and Table IIA). A similar increase in neomycin affinity has been reported for R54E and R176A when co-expressed with SUR2A (Schulze *et al*, 2003), rather than SUR1. The increased neomycin affinity suggests that these mutant channels bind PIP₂ less strongly, so that less neomycin is required to chelate bound PIP₂. In agreement with this idea, the ability of the soluble PIP₂ analogue diC₈-PIP₂ (25 μ M) to activate the mutant channels immediately after patch excision was increased from 2.5-fold for wild-type Kir6.2/SUR1 to 5-fold for R54L, 6-fold for K67L and 7-fold for both R54E and R176A (Figure 7A and Table IIA). We presume this is because wild-type channels are already almost fully activated by endogenous PIP₂. Following rundown of channel activity, however, wild-type channels were activated as potently (Table IIA). These functional studies are in agreement with the modelling studies (see above), which predicted loss of PIP₂ binding following mutation of R54, K67 and R176.

We also tested the effect of mutations at R50 on both neomycin block and diC₈-PIP₂ activation. Charge neutralisation (R50Q) or reversal (R50E) had no effect on either neomycin block or diC₈-PIP₂ activation of either Kir6.2DC or Kir6.2/SUR1 (Table IIA and B). These data indicate that residue R50 does not form part of the PIP₂-binding site itself, consistent with our model. We also examined whether the ability of diC₈-PIP₂ to activate channels blocked by ATP was altered by mutation of R50, as might be expected if the presence of PIP₂ in its binding site electrostatically influences the position of R50 (as suggested by our simulations). However, activation of ATP-blocked R50Q and R50E channels was not less than wild type (Supplementary Figure 1).

A cysteine residue at position 42 also lies within 4.5 Å of PIP₂ and its mutation causes neonatal diabetes (Yorifuji *et al*, 2005). There was no effect of mutating C42 to arginine or glutamate on neomycin sensitivity (data not shown), which is in agreement with the fact that it is the backbone of C42 that lines the PIP₂-binding site. However, Kir6.2-C42R/SUR1 channels had an increased intrinsic *P*_o and ran down rapidly in excised patches making them difficult to study.

The IC₅₀ for neomycin inhibition of Kir6.2 Δ C was greater than that of Kir6.2/SUR1 channels (80 versus 26 μ M; Figure 6B and Table II), indicating that the channel binds PIP₂ more effectively in the absence of SUR1. An increase in

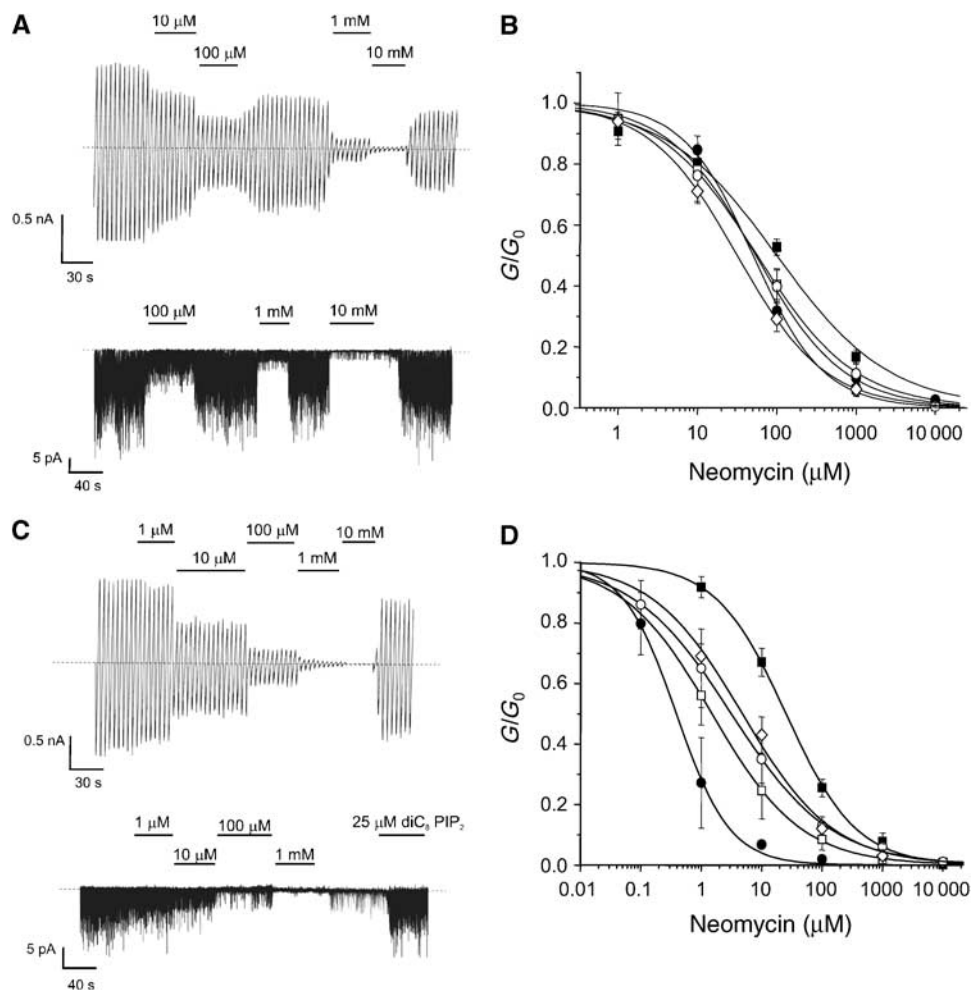


Figure 6 (A) above, K_{ATP} currents elicited by voltage ramps from -110 to $+100$ mV applied to an inside-out patch excised from a *Xenopus* oocyte expressing Kir6.2 Δ C. below, Kir6.2 Δ C-R176A currents recorded from an inside-out patch at a holding potential of -60 mV. The dotted line indicates the zero current level. Bars indicate addition of neomycin. (B) Mean relationship between neomycin concentration and K_{ATP} conductance (G), expressed relative to the conductance in the absence of neomycin (G_0) for Kir6.2 Δ C (filled squares), Kir6.2 Δ C-R54E (open circles), Kir6.2 Δ C-R54L (open diamonds), Kir6.2 Δ C-K67L (filled circles) or Kir6.2 Δ C-R176A (open squares) channels. The curves are the best fit to equation 1. (C) K_{ATP} currents elicited by voltage ramps from -110 to $+100$ mV applied to an inside-out patch excised from a *Xenopus* oocyte expressing Kir6.2/SUR1 (above). Kir6.2-R176A/SUR1 currents recorded from an inside-out patch at a holding potential of -60 mV (below). The dotted line indicates the zero current level. Bars indicate addition of neomycin. (D) Mean relationship between neomycin concentration and K_{ATP} conductance (G), expressed relative to the conductance in the absence of neomycin (G_0) for SUR1 coexpressed with Kir6.2 (filled squares), Kir6.2-R54E (open circles), Kir6.2-R54L (open diamonds), Kir6.2-K67L (filled circles) or Kir6.2-R176A (open squares). The curves are the best fit to equation 1.

the IC_{50} for neomycin inhibition was also observed for the R54E, R54L, R176A and K67L mutations in Kir6.2 Δ C (Figure 4B and Table IIB). However, the shift was less than that found when mutant Kir6.2 was coexpressed with SUR1. DiC₈-PIP₂ activated wild-type and mutant Kir6.2 Δ C channels in a similar way to Kir6.2/SUR1 channels (Figure 7B and Table IIB).

Discussion

The PIP₂-binding site

Our model predicts that there are four PIP₂-binding sites in the Kir6.2 tetramer, one per subunit. The negatively charged PIP₂ head group is coordinated by a cloud of positively charged residues, and is anchored just below the plane of the membrane by the lipid tails of the molecule. Both the N- and C-terminal domains of Kir6.2 contribute to the PIP₂-binding site, as suggested by functional studies (Fan and

Makielski, 1997; Shyng *et al*, 2000; Cukras *et al*, 2002; MacGregor *et al*, 2002; Schulze *et al*, 2003). Like the ATP-binding site (Antcliff *et al*, 2005), the PIP₂-binding site lies at the interface between two neighbouring subunits. Most residues are contributed by the N and C termini of the same subunit, but there are additional contributions from the N terminus of the adjacent subunit. Positioning of the ligand-binding site at the subunit interface appears to be a common theme in ion channels (Ashcroft, 2006) and likely serves to precipitate a larger, coordinated conformational change in the whole channel on ligand binding.

N-terminal residues that lie close to PIP₂ include K39 and K67 on the same subunit and R54 on the adjacent subunit. The former is of special interest as it also forms part of the ATP-binding site, the side chain interacting with the PIP₂ headgroup and the backbone with ATP. Mutation of K67 to alanine reduced the P_o (Cukras *et al*, 2002), as expected if it interacts with PIP₂. Furthermore, as we show here, mutation

Table II Neomycin and diC₈-PIP₂ sensitivity of wild-type and mutant K_{ATP} channels

Mutation	<i>I</i> _{excision} (pA)	Neomycin IC ₅₀ (μM)	Fold activation by diC ₈ -PIP ₂	
			After excision	After rundown
<i>A: Kir6.2/SUR1</i>				
WT	1265 ± 125 (7)	26 ± 5 (6)	2.5 ± 0.7 (9)	8.9 ± 3.3 (6)
R54E	14 ± 4 (20)	5.5 ± 1.7 (7)	6.5 ± 1.9 (14)	4.5 ± 1.0 (11)
R54L	—	5.7 ± 1.43 (7)	5.3 ± 1.7 (7)	6.4 ± 2.1 (7)
K67L	6 ± 3 (6)	0.7 ± 0.4 (3)	5.7 ± 2.3 (5)	0.5 ± 0.1 (4)
R176A	9 ± 2 (8)	2.2 ± 0.8 (5)	6.9 ± 2.8 (6)	6.6 ± 1.1 (4)
R50E	—	21 ± 4 (6)	1.1 ± 0.1 (6)	3.6 ± 1.0 (6)
R50Q	—	69 ± 17 (6)	2.6 ± 0.1 (6)	3.7 ± 1.1 (6)
<i>B: Kir6.2ΔC36</i>				
WT	908 ± 150 (11)	97 ± 13 (16)	1.3 ± 0.1 (10)	3.3 ± 0.4 (11)
R54E	3.5 ± 0.4 (9)	51 ± 14 (7)	3.5 ± 1.1 (8)	1.6 ± 0.3 (5)
R54L	—	30 ± 5 (8)	3.1 ± 0.8 (8)	11.2 ± 2.8 (8)
K67L	2.7 ± 0.4 (7)	51 ± 7 (7)	13.1 ± 6.4 (7)	1.5 ± 0.3 (5)
R176A	2.4 ± 0.3 (5)	64 ± 20 (5)	7.6 ± 6.0 (5)	0.7 ± 0.1 (4)
R50E	—	92 ± 20 (6)	1.8 ± 0.4 (6)	3.2 ± 0.7 (6)
R50Q	—	93 ± 21 (8)	1.7 ± 0.3 (8)	2.5 ± 0.6 (8)

WT, wild-type. Numbers in parentheses indicate the number of oocytes.

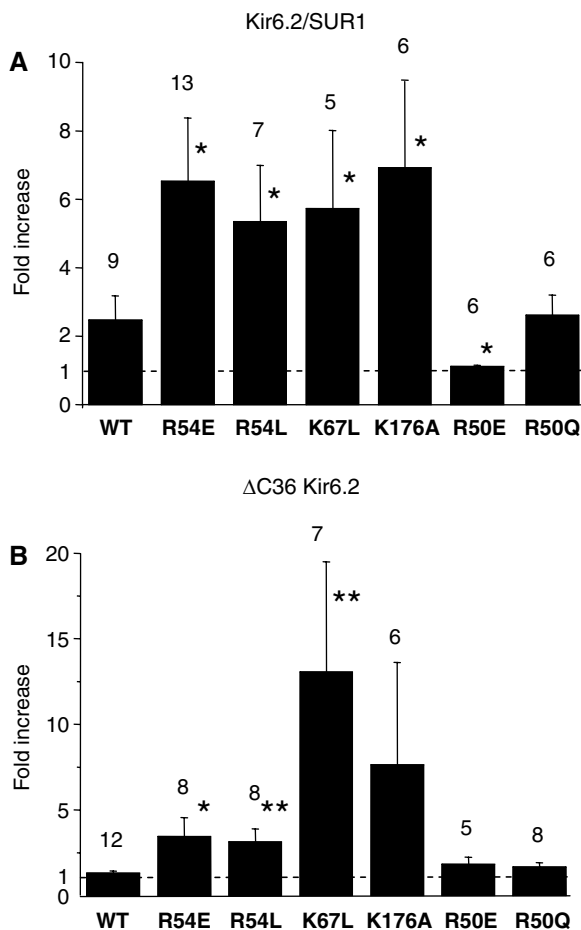


Figure 7 (A, B) Activation of wild-type and mutant K_{ATP} channels, as indicated, by 25 μM diC₈-PIP₂. The number of patches is indicated above the bar. Statistical significance against wild-type is indicated (Mann–Whitney *U*-test): *P* < 0.05 (*), *P* < 0.01 (**).

to glutamate enhances neomycin binding, indicative of a lower affinity for PIP₂. However, neither K67N nor K67E altered the channel ATP sensitivity nor the ability of PIP₂ to

modulate ATP inhibition (Reimann *et al*, 2003; Schulze *et al*, 2003). This may be explained by the exponential relationship between *P*_o and the IC₅₀ for ATP inhibition, which predicts that changes in *P*_o have a measurable effect on ATP sensitivity only when *P*_o is greater than 0.7 (Enkvetchakul *et al*, 2000). Mutations at R54 impair PIP₂ modulation in a manner consistent with the idea that R54 interacts electrostatically with the phospholipid (Schulze *et al*, 2003; this paper), as our model predicts.

In the C terminus, our model indicates R176, R177, E179 and R301 lie close to PIP₂. Of these residues, R176, R177 and R301 have been shown to confer a reduced PIP₂ sensitivity when mutated to alanine, as evidenced by a smaller intrinsic *P*_o and a reduced activation when exposed to PIP₂ (Fan and Makielski, 1997; Shyng *et al*, 2000). All three residues lie in close proximity to the phosphate groups on PIP₂ and R176 and R301 make direct interactions with it. Although several mutations at E179 in Kir6.2ΔC (e.g. Q,M,L) do not alter the single-channel kinetics, mutation to asparagine dramatically increased the *P*_o (Antcliff *et al*, 2005).

PIP₂ binding and human disease

A number of mutations in Kir6.2 that cause neonatal diabetes have been identified (Ashcroft, 2005). Among the residues that lie close to PIP₂, only mutations at C42 and E179 have been found to cause diabetes to date (Yorifuji *et al*, 2005). As E179 lies in the ATP-binding site, it may influence ATP binding directly (Antcliff *et al*, 2005). The C42R mutation results in a substantial increase in *P*_o (Yorifuji *et al*, 2005; see above), suggesting that it might act by enhancing PIP₂ binding. Our studies showed that this was not the case as neomycin sensitivity was unaffected; however, this is consistent with the fact that in the model the backbone rather than the side chain of C42 lines the PIP₂-binding pocket.

Congenital hyperinsulinism (CHI) is also associated with mutation of Kir6.2 residues that lie close to the putative PIP₂-binding site, including F55L, K67N and R301H (Reimann *et al*, 2003; Gloyn *et al*, 2006; Lin *et al*, 2006). All CHI mutations reduce the beta-cell K_{ATP} current and thereby stimulate insulin secretion (Ashcroft, 2005). The F55L

mutation produces a markedly decreased P_o , which can be partially reversed by PIP₂, suggesting it may act by decreasing PIP₂ sensitivity (Lin *et al*, 2006). Conceivably, F55 might interact with the lipid tails of PIP₂, as a hydrophobic residue is required at this position. Alternatively, the F55L mutation might exert its effect allosterically, by modifying the position of R54 (which interacts with PIP₂ and strongly reduces channel activity when mutated; Schulze *et al*, 2003).

In the case of K67N and R301H, we speculate that the loss of a positive charge at these positions may destabilise PIP₂ binding, leading to a decrease in P_o and thereby impaired insulin secretion. Their location within 4.5 Å of the negatively charged phosphate groups of PIP₂ in our model is harmonious with this idea. When R301 is mutated to glutamate, no functional channels are observed (Shyng *et al*, 2000), consistent with the idea that this mutation destabilises PIP₂ binding, thus causing the channel to remain closed. When R301 was mutated to alanine, channels ran down very rapidly in excised patches (Shyng *et al*, 2000). Addition of PIP₂ produced a much larger and slower response than found for wild-type channels, again suggesting that PIP₂ binding was reduced.

Interactions with ATP

PIP₂ has two effects on the K_{ATP} channel: it increases P_o (as discussed above) and it reduces ATP inhibition. The proximity of the PIP₂-binding site to the slide helix suggests a mechanism by which it may influence P_o , as the slide helix is believed to play a key role in channel gating (Kuo *et al*, 2003) and mutations in this domain influence P_o (Ashcroft, 2005). The close location of the ATP- and PIP₂-binding sites in our model is also consistent with the idea that these ligands influence the binding of each other electrostatically (Fan and Makielski, 1999). Precisely, how PIP₂ displaces ATP binding remains unresolved. However, some residues are shared by both PIP₂- and ATP-binding sites (K39, E179 and R301), so that binding of one ligand could conceivably perturb the binding site for the other.

The phosphate tail of ATP interacts with R50, K185 and R201. Mutations at R201 cause a marked reduction in K_{ATP} channel ATP sensitivity (John *et al*, 2003) and are a common cause of neonatal diabetes (Ashcroft, 2005). Functional studies have concluded, however, that neither R50 nor R201 interact with PIP₂ (Schulze *et al*, 2003; Ribalet *et al*, 2005; this paper). The MD simulations, however, suggest that interaction of R50, R201 and eventually K185 are reduced in the presence of PIP₂. Most dramatically, the presence of PIP₂ causes R50 to move. This would be expected to reduce ATP binding and would suggest that neutralisation or reversal of the charge at R50 might abolish this effect. However, in functional studies, we could find no evidence that mutation of R50 reduced the ability of PIP₂ to decrease the channel ATP sensitivity. This discrepancy suggests to us that PIP₂ binding may induce a substantial conformational change in the channel that is not captured in the MD simulations (because it occurs on a longer time scale), and that this conformational change removes R50 from the influence of PIP₂. Indeed, substantial changes in the conformation of KirBac3.1 are suggested by 2D electron microscope projection images of the open and closed state. (Kuo *et al*, 2005).

Methodological limitations

One limitation of the current study is the use of a rigid protein model in the docking calculations. This may result in some sensitivity of the docking result to the protein side-chain rotamers and to the local backbone conformation. Only limited relaxation of side chain and backbone conformations at the binding site will be possible in the presence of bound ligand on a 10-ns timescale. Future studies will address the influence of side chain and local backbone flexibility on Kir6.2–ligand interactions, for example, by combining replica exchange MD simulations of the apo-state of the protein (i.e., in the absence of bound ligand) with docking to multiple conformations generated by the MD simulations.

Effects of other phospholipids

Whereas PIP₂ and PIP₃ have marked effects on Kir6.2/SUR channels, PIP is less effective and PI and inositol have no effect (Fan and Makielski, 1997; Baukowitz *et al*, 1998; Shyng and Nichols, 1998). Likewise, recombinant Kir6.2 is able to bind various PIP₂ isomers, as well as PIP₃ and PIP, but not IP₃ or PI (Wang *et al*, 2002). The lack of effect of the isolated head group (IP₃) may be because the lipid tail localises PIP₂ to the membrane and ensures a high concentration of the charged head group in the vicinity of the channel. Alternatively, the lipid tail may be required to anchor the head group in the correct position. The fact that the number of negative charges is important suggests an electrostatic effect, and is consistent with the electrostatic interactions observed in our model. Polyvalent cations reverse the effects of PIP₂, presumably by chelating the amount of the charged head group in the membrane.

Short acyl chain PIP₂ analogues are much less able to activate Kir channels (Kir2.1, 3.1/3.4). For example, diC₄-PIP₂ was ineffective, whereas diC₈-PIP₂ quickly and reversibly activated Kir channels (Rohacs *et al*, 2003; Figure 7). Our model suggests this is because the shorter tail prevents the charged head group from accessing its binding site.

Comparison with previous models for the PIP₂-binding site

A previous study has argued that residues E308, I309, W311 and F315 are critical for PIP₂ interactions, as mutations at these residues abolished channel activity and it could not be recovered by PIP₂ (Cukras *et al*, 2002). However, expression levels and membrane association were also reduced, suggesting these residues may also be important in Kir6.2 stability and surface trafficking. Our model indicates this is the more likely explanation, as all these residues lie distant from the PIP₂-binding site, and too far below the plane of the membrane for the PIP₂ molecule to span the gap. Other residues that have been implicated in interaction with PIP₂ are R314 and E229 (Lin *et al*, 2003). However, these residues are involved in salt-bridge formation between subunits. Their effects must therefore be allosteric and mediated via changes in P_o .

PIP₂ also diminished channel activation by K⁺ channel openers and reduced inhibition by sulphonylureas (Krauter *et al*, 2001). This effect can be attributed to the action of the phosphoinositide on P_o . An increase in P_o will indirectly reduce inhibition by both sulphonylureas and ATP, as these ligands stabilise the long closed state of the channel, which is entered less frequently (Trapp *et al*, 1998; Enkvetchakul *et al*,

2000). When P_o is high, the effect of K channel openers is also effectively reduced, because it is impossible to increase P_o above unity.

Comparison with other Kir channels

Several residues that line the putative PIP₂-binding pocket are highly conserved among Kir channels, including R54, K67, R176, R177 and R301. Functional studies also suggest that the PIP₂-binding site may be conserved across Kir channels. For example, neutralisation of the charge at the residue equivalent to R177 in Kir6.2 reduces PIP₂ binding in Kir1.1 (Huang *et al*, 1998). In Kir2.1, residues equivalent to K38, N41, R54, Q173, H174, R175, R176, R206, K207, H216 and R301 interact functionally with PIP₂, and R206 and R301 cause Anderson's syndrome when mutated (Lopes *et al*, 2002). Several of these residues contribute to the putative PIP₂-binding site of Kir6.2 (N41, R54, R176, R301), or lie immediately adjacent to residues that do so (K38, R175). Furthermore, rotation of the side chains would bring residues R206 and K207 close enough to the PIP₂ headgroup to make electrostatic interactions. These data suggest that the PIP₂-binding site may be similar in other Kir channels.

Some Kir channels discriminate between different phosphoinositides. For example, Kir1.1 shows a marked specificity for PIP₂ with phosphates at positions 4 and 5 (Rohacs *et al*, 1999). In contrast, Kir6.2 is promiscuous. We attempted docking of PI(3,4)P₂ and PI(3,4,5)P₂, but found that these compounds bound less effectively than PIP₂. This lack of agreement with the functional studies may reflect the fact the model does not permit flexibility of the side chains during the docking procedure (see model limitations above). The most favoured conformation adopted by PI(3,4)P₂ is the one in which the phosphate in the third position points towards K67. Although K67 is rather distant to form a strong interaction in the model, it is likely that if K67 is allowed to move (which our model does not allow), it would interact with the phosphate at the third position. This could enhance binding. Thus, we favour the idea that the lack of PI(3,4)P₂ binding in our model is due to the limitation of the fixed protein side-chain algorithm. Second, our model does not include the first 30 amino acids of Kir6.2, as there is no structural information on which to model them. It is possible that these residues may contribute to binding of PI(3,4,5)P₂ and PI(3,4)P₂. Finally, there may be minor differences between the predicted and actual PIP₂-binding site. For example, the orientation of a single side chain could impair binding of PIPs with a phosphate at position 3 of PIP₂. However, it is unlikely that our model is grossly incorrect, as it is in excellent agreement with all the functional and mutagenesis data on channel regulation by both ATP and PI(4,5)P₂.

Interestingly, Kir2.1 has an aspartate at the position equivalent to K39 in Kir6.2, and its mutation to a lysine renders Kir2.1 sensitive to PI3,4,5P₂, like Kir6.2 (Rohacs *et al*, 1999). This may reflect the fact that, in our model, K39 interacts with P4 of the IP₃ headgroup. Thus, relatively minor differences in structure can account for differences in phosphoinositide binding. This strengthens the argument that our model of the PIP₂-binding site is applicable to other eukaryotic Kir channels.

In contrast to eukaryotic Kir channels, KirBac1.1 is blocked by PIP₂ (Enkvetchakul *et al*, 2005). Despite this, the dependence on the number of phosphate groups and a lipid tail is

similar. This further suggests that the PIP₂-binding site of prokaryotic Kir channels may be largely similar to that we propose for Kir6.2, and that differences in the way binding is coupled to channel gating account for the opposite actions of PIP₂ in prokaryotic and eukaryotic Kir channels.

Materials and methods

Computational studies

The sequences were taken from GenBank (<http://www.ncbi.nlm.nih.gov/Genbank/>) and aligned using ClustalX (Chenna *et al*, 2003). Models of Kir6.2 were generated using Modeller v6.2 (<http://salilab.org/modeller/>) (Sanchez and Sali, 2000) using the X-ray crystal structures of a bacterial inward rectifier KirBac1.1 (PDB code 1P7B) and the IC domain of a rat inward rectifier Kir3.1 (PDB code 1N9P) as templates. Several models were generated, with the final one being selected based on the internal ranking criteria within the programme and also on the low C α RMSD value after superimposing on the template structures. The generation of the model is described in detail elsewhere (Antcliff *et al*, 2005; Haider *et al*, 2007). Several rounds of energy minimisation were carried out to obtain a final low-energy conformation with no steric clashes between side chains. The final C α RMSD between the template and the model was 0.4 Å for the N domain, 1.7 Å for the slide helix and the transmembrane domains, and 1.3 Å for the C domain.

The PIP₂-binding site was identified by automated ligand docking using the programme AUTODOCK v3.0.5 (<http://autodock.scripps.edu/>) (Goodsell *et al*, 1996), which employs a Monte Carlo simulated annealing algorithm. This programme allows the ligand to be flexible, whereas the protein side chains remain fixed. The parameterisation of PIP₂ was generated from the ProDrg (van Aalten *et al*, 1996) server (<http://davapc1.bioch.dundee.ac.uk/programs/prodrg/>) and used as a direct input in the AUTODOCK programme. Only the IP₃ head group of the PIP₂ molecule was used in the docking protocol; the long acyl hydrophobic tails were omitted due to the presence of a high number of rotational bonds and the reasons mentioned above. DefTors within AUTODOCK was used to identify 12 rotatable bonds in the IP₃ molecule that were allowed to be flexible and not restrained during docking. A grid of 210 × 210 × 80 points was generated with a grid spacing of 0.375 Å around the central positively charged region, which corresponded to a volume space of 182 520 Å³. This grid space defines the region of the protein in which the ligand searched for the most favourable interactions. The partial charges were assigned semi-empirically using MOPAC in the Insight suite of programs (www.accelrys.com). A total of 200 dockings were carried out with 5000 cycles per run; interaction energies were calculated for various docked positions and ranked in accordance with the interaction energies between the ligand and the protein. From these top 50 solutions, the final conformation of the docked IP₃ head group was identified on the basis of the orientation, distance from the membrane and interaction energies.

Once the residues that contributed to the binding site were identified, the complex (IP₃ + Kir6.2) was subjected to short bursts of energy minimisation to allow IP₃ to settle into its binding site. The quality of the model was assessed at each step and the stereochemical properties monitored strictly using PROCHECK v3.4.4 (Laskowski *et al*, 1993). The Kir6.2-PIP₂ model was compared with that of Kir6.2 with docked ATP (Haider *et al*, 2007). A third model of Kir6.2 was generated in which both ATP and PIP₂ were present simultaneously in their respective binding sites. This was achieved by superimposing one system over the other, extracting the coordinates for ATP and placing ATP in its binding site in the Kir6.2-PIP₂ model. Thus, four models were used in this study: model 1 = Kir6.2 + PIP₂; model 2 = Kir6.2 + ATP; model 3 = Kir6.2 + ATP + PIP₂; model 4 = Kir6.2.

The molecular models of Kir6.2 + PIP₂ and Kir6.2 + ATP + PIP₂ were embedded in a POPC bilayer of ~35 Å thickness (Faraldo-Gomez *et al*, 2002). Two K⁺ ions were positioned in the selectivity filter at S1 and S3 positions. These were interspaced with water molecules at positions S0, S2 and S4 as observed in the crystal structures. The central cavity of the channel was solvated using the programs Voidoo (Kleywegt and Jones, 1994) and Flood. The resulting system was then solvated with SPC molecules and neutralised by counter ions that were added at random positions

to the bulk solvent. This generated a system of ~99 000 atoms. The system was energy minimised for 1000 steps of steepest descents, following which 0.25 ns of molecular dynamics was carried out to equilibrate the system. The protein atoms along with the ligand were harmonically restrained using a force constant of 1000 kJ/mol/nm². The ions and the solvent molecules were allowed to move during the equilibration process. After the initial equilibration, the restraints were removed from the complex and the systems were allowed to a 10 ns production run.

Molecular dynamics simulations were carried out using GROMACS v3.1.4 (www.gromacs.org) (Lindahl *et al*, 2001) (with the GROMOS87 forcefield). The simulations employed Berendsen coupling (Berendsen *et al*, 1984) to maintain a constant temperature of 300 K and a constant isotropic pressure of 1 Bar. Van der Waals interactions were modelled using Lennard-Jones 6–12 potentials with a 1.3-nm cut-off. Long-range electrostatic interactions were calculated using Particle Mesh Ewald method (Darden *et al*, 1993), with a cut-off for the real space term of 1.2 nm. Covalent bonds were constrained using the LINCS algorithm (Hess *et al*, 1997). The time step employed was 2 fs and the coordinates were saved every 10 ps for analysis. Analysis of the simulations was carried out using the programs in the GROMACS suite of packages and local scripts. Molecular graphics images were generated using VMD (Humphrey *et al*, 1996).

Functional studies

Mouse Kir6.2 (Genbank D50581) and rat SUR1 (Genbank L40624) were used in this study. Site-directed mutagenesis of Kir6.2 and preparation of mRNAs was as described previously (Trapp *et al*, 1998). *Xenopus laevis* oocytes were injected with 0.1 ng wild-type or mutant Kir6.2 and ~2 ng of SUR1 mRNAs (giving a 1:20 ratio), and studied 1–4 days later (Trapp *et al*, 1998). In some experiments, oocytes were injected with 0.1 ng wild-type or mutant Kir6.2ΔC, a C-terminally truncated version of Kir6.2 that expresses in the absence of SUR (Tucker *et al*, 1997).

Macroscopic currents were recorded from giant excised inside-out patches using the patch-clamp technique in response to 3 s voltage ramps from –110 mV to +100 mV (holding potential, 0 mV)

References

Antcliff JF, Haider S, Proks P, Sansom MSP, Ashcroft FM (2005) Functional analysis of a structural model of the ATP-binding site of the K_{ATP} channel Kir6.2 subunit. *EMBO J* **24**: 229–239

Ashcroft FM (2005) ATP-sensitive potassium channelopathies: focus on insulin secretion. *J Clin Invest* **115**: 2047–2058

Ashcroft FM (2006) Ion channels and disease: from molecule to malady. *Nature* **440**: 440–447

Baukowitz T, Schulte U, Oliver D, Herlitz S, Krauter T, Tucker SJ, Ruppersberg JP, Fakler B (1998) PIP₂ and PIP as determinants for ATP inhibition of K_{ATP} channels. *Science* **282**: 1141–1144

Berendsen HJC, Postma JPM, van Gunsteren WF, DiNola A, Haak JR (1984) Molecular dynamics with coupling to an external bath. *J Chem Phys* **81**: 3684–3690

Capener CE, Shrivastava IH, Ranatunga KM, Forrest LR, Smith GR, Sansom MSP (2000) Homology modelling and simulation of an inward rectifier potassium channel. *Biophys J* **78**: 2929–2942

Chenna R, Sugawara H, Koike T, Lopez R, Gibson TJ, Higgins DG, Thompson JD (2003) Multiple sequence alignment with the Clustal series of programs. *Nucleic Acids Res* **31**: 3497–3500

Cukras CA, Jeliakova I, Nichols CG (2002) Structural and functional determinants of conserved lipid interaction domains of inward rectifying Kir6.2 channels. *J Gen Physiol* **119**: 581–591

Darden T, York D, Pedersen L (1993) Particle mesh Ewald—an N.log(N) method for Ewald sums in large systems. *J Chem Phys* **98**: 10089–10092

Enkvetchakul D, Jeliakova I, Nichols CG (2005) Direct modulation of Kir channel gating by membrane phosphatidylinositol 4,5-bisphosphate. *J Biol Chem* **280**: 35785–35788

Enkvetchakul D, Loussouarn G, Makhina E, Shyng SL, Nichols CG (2000) The kinetic and physical basis of K_{ATP} channel gating: toward a unified molecular understanding. *Biophys J* **78**: 2334–2348

Fan Z, Makielski JC (1997) Anionic phospholipids activate ATP-sensitive potassium channels. *J Biol Chem* **272**: 5388–5395

at 20–24°C. Currents were filtered at 0.15 kHz and digitised at 0.5 kHz. For R54E, R176A, K67L Kir6.2 channel currents were recorded from giant inside-out patches at a holding potential of –60 mV and 20–24°C. The currents were filtered at 2 kHz, digitised at 5 kHz using a Digidata 1320 Interface and analysed using pClamp9.2 software (Axon Instruments). The pipette solution contained (mM): 120 KCl, 1.8 CaCl₂, 10 HEPES (pH 7.2 with KOH). The internal solution contained (mM): 100 KCl, 2 EGTA, 10 HEPES (pH 7.2 with KOH) and neomycin as indicated. Neomycin was obtained from Sigma. Synthetic dioctanoyl phosphatidylinositol (4,5) bisphosphate (diC₈-PIP₂) was purchased from Echelon Bioscience Inc. (Salt Lake City, UT) and dissolved in internal solution to make a 1 mM stock, which was stored as aliquots at –80°C. Rapid exchange of internal solutions was achieved using a sewer-pipe system.

To control for possible rundown, the control conductance (G₀) was taken as the mean of that in control solution before and after neomycin application. Neomycin concentration-response curves were fit by the Hill equation (equation 1):

$$G/G_0 = 1/(1 + ([N]/IC_{50})^h), \quad (1)$$

where [N] is the neomycin concentration, IC₅₀ is the concentration at which inhibition is half maximal and *h* is the Hill coefficient. All data are given as mean ± s.e.m. Statistical significance was tested by Mann–Whitney *U*-test.

Supplementary data

Supplementary data are available at *The EMBO Journal* Online (<http://www.embojournal.org>).

Acknowledgements

We thank the Wellcome Trust (MS, FMA), the European Union (EURODIA, BIOSIM; FMA) and the Royal Society (FMA) for support. This work is an OXION collaboration. FMA is a Royal Society Research Professor. We have no financial conflicts of interest.

Fan Z, Makielski JC (1999) Phosphoinositides decrease ATP sensitivity of the cardiac ATP-sensitive K(+) channel. A molecular probe for the mechanism of ATP-sensitive inhibition. *J Gen Physiol* **114**: 251–269

Faraldo-Gomez JD, Smith GR, Sansom MSP (2002) Setting up and optimization of membrane protein simulations. *Eur Biophys J* **31**: 217–227

Gloyn AL, Siddiqui J, Ellard S (2006) Mutations in the genes encoding the pancreatic beta-cell K_{ATP} channel subunits Kir6.2 (KCNJ11) and SUR1 (ABCC8) in diabetes mellitus and hyperinsulinism. *Hum Mutat* **27**: 220–231

Goodsell DS, Morris GM, Olson AJ (1996) Automated docking of flexible ligands: applications of AutoDock. *J Mol Recog* **9**: 1–5

Haider S, Antcliff JF, Proks P, Sansom MSP, Ashcroft FM (2005a) Focus on Kir6.2: a key component of the ATP-sensitive potassium channel. *J Mol Cell Cardiol* **38**: 927–936

Haider S, Grottesi A, Hall BA, Ashcroft FA, Sansom MSP (2005b) Conformational dynamics of the ligand-binding domain of inward rectifier K channels as revealed by molecular dynamics simulations: towards understanding Kir channel gating. *Biophys J* **88**: 3310–3320

Haider S, Khalid S, Tucker SJ, Ashcroft FM, Sansom MS (2007) Molecular dynamics simulations of inwardly rectifying (Kir) potassium channels: a comparative study. *Biochemistry* **46**: 3643–3652

Hess B, Bekker H, Berendsen HJC, Fraaije JGEM (1997) LINCS: a linear constraint solver for molecular simulations. *J Comp Chem* **18**: 1463–1472

Holyoake J, Caulfield V, Baldwin SA, Sansom MSP (2006) Modelling, docking and simulation of the major facilitator superfamily. *Biophys J* **91**: L84–L86

Huang CL, Feng S, Hilgemann DW (1998) Direct activation of inward rectifier potassium channels by PIP₂ and its stabilization by Gbetagamma. *Nature* **391**: 803–806

- Humphrey W, Dalke A, Schulten K (1996) VMD—visual molecular dynamics. *J Molec Graph* **14**: 33–38
- John SA, Weiss JN, Xie LH, Ribalet B (2003) Molecular mechanism for ATP-dependent closure of the K⁺ channel Kir6.2. *J Physiol* **552**: 23–34
- Kleywegt GJ, Jones TA (1994) Detection, delineation, measurement and display of cavities in macromolecular structures. *Acta Crystallogr D* **50**: 178–185
- Krauter T, Ruppertsberg JP, Baukowitz T (2001) Phospholipids as modulators of K_{ATP} channels: distinct mechanisms for control of sensitivity to sulphonylureas, K⁺ channel openers, and ATP. *Mol Pharmacol* **59**: 1086–1093
- Kuo A, Domene C, Johnson LN, Doyle DA, Venien-Bryan C (2005) Two different conformational states of the KirBac3.1 potassium channel revealed by electron crystallography. *Structure* **13**: 1463–1472
- Kuo A, Gulbis JM, Antcliff JF, Rahman T, Lowe ED, Zimmer J, Cuthbertson J, Ashcroft FM, Ezaki T, Doyle DA (2003) Crystal structure of the potassium channel KirBac1.1 in the closed state. *Science* **300**: 1922–1926
- Laskowski RA, MacArthur MW, Moss DS, Thornton JM (1993) Procheck—a program to check the stereochemical quality of protein structures. *J Appl Cryst* **26**: 283–291
- Law RJ, Capener C, Baaden M, Bond PJ, Campbell J, Patargias G, Arinaminpathy Y, Sansom MSP (2005) Membrane protein structure quality in molecular dynamics simulation. *J Mol Graph Mod* **24**: 157–165
- Lin YW, Jia T, Weinsoft AM, Shyng SL (2003) Stabilization of the activity of ATP-sensitive potassium channels by ion pairs formed between adjacent Kir6.2 subunits. *J Gen Physiol* **122**: 225–237
- Lin YW, MacMullen C, Ganguly A, Stanley CA, Shyng SL (2006) A novel KCNJ11 mutation associated with congenital hyperinsulinism reduces the intrinsic open probability of beta-cell ATP-sensitive potassium channels. *J Biol Chem* **281**: 3006–3012
- Lindahl E, Hess B, van der Spoel D (2001) GROMACS 3.0: a package for molecular simulation and trajectory analysis. *J Molec Model* **7**: 306–317
- Lopes CM, Zhang H, Rohacs T, Jin T, Yang J, Logothetis DE (2002) Alterations in conserved Kir channel-PIP₂ interactions underlie channelopathies. *Neuron* **34**: 933–944
- MacGregor GG, Dong K, Vanoye CG, Tang L, Giebisch G, Hebert SC (2002) Nucleotides and phospholipids compete for binding to the C terminus of K_{ATP} channels. *Proc Natl Acad Sci USA* **99**: 2726–2731
- Nishida M, MacKinnon R (2002) Structural basis of inward rectification: cytoplasmic pore of the G protein-gated inward rectifier GIRK1 at 1.8 Å resolution. *Cell* **111**: 957–965
- Pegan S, Arrabit C, Zhou W, Kwiatkowski W, Collins A, Slesinger PA, Choe S (2005) Cytoplasmic domain structures of Kir2.1 and Kir3.1 show sites for modulating gating and rectification. *Nat Neurosci* **8**: 279–287
- Reimann F, Huopio H, Dabrowski M, Proks P, Gribble FM, Laakso M, Otonkoski T, Ashcroft FM (2003) Characterization of new K_{ATP}-channel mutations associated with congenital hyperinsulinism in the Finnish population. *Diabetologia* **46**: 241–249
- Ribalet B, John SA, Xie LH, Weiss JN (2005) Regulation of the ATP-sensitive K channel Kir6.2 by ATP and PIP₂. *J Mol Cell Cardiol* **39**: 71–77
- Rohacs T, Chen J, Prestwich GD, Logothetis DE (1999) Distinct specificities of inwardly rectifying K⁺ channels for phosphoinositides. *J Biol Chem* **274**: 36065–36072
- Rohacs T, Lopes CM, Jin T, Ramdya PP, Molnar Z, Logothetis DE (2003) Specificity of activation by phosphoinositides determines lipid regulation of Kir channels. *Proc Natl Acad Sci USA* **100**: 745–750
- Sakura H, Ämmälä C, Smith PA, Gribble FM, Ashcroft FM (1995) Cloning and functional expression of the cDNA encoding a novel ATP-sensitive potassium channel expressed in pancreatic β-cells, brain, heart and skeletal muscle. *FEBS Lett* **377**: 338–344
- Sanchez R, Sali A (2000) Comparative protein structure modeling. Introduction and practical examples with Modeller. *Methods Mol Biol* **143**: 97–129
- Sansom MSP, Bond PJ, Deol SD, Grottesi A, Haider S, Sands ZA (2005) Molecular simulations and lipid/protein interactions: potassium channels and other membrane proteins. *Biochem Soc Transac* **33**: 916–920
- Schulze D, Krauter T, Fritzenschaft H, Soom M, Baukowitz T (2003) Phosphatidylinositol 4,5-bisphosphate (PIP₂) modulation of ATP and pH sensitivity in Kir channels. A tale of an active and a silent PIP₂ site in the N terminus. *J Biol Chem* **278**: 10500–10505
- Shyng SL, Cukras CA, Harwood J, Nichols CG (2000) Structural determinants of PIP₂ regulation of inward rectifier K_{ATP} channels. *J Gen Physiol* **116**: 599–608
- Shyng SL, Nichols CG (1998) Membrane phospholipid control of nucleotide sensitivity of K_{ATP} channels. *Science* **282**: 1138–1141
- Trapp S, Proks P, Tucker SJ, Ashcroft FM (1998) Molecular analysis of K_{ATP} channel gating and implications for channel inhibition by ATP. *J Gen Physiol* **112**: 333–349
- Tucker SJ, Gribble FM, Zhao C, Trapp S, Ashcroft FM (1997) Truncation of Kir6.2 produces ATP-sensitive K-channels in the absence of the sulphonylurea receptor. *Nature* **387**: 179–183
- van Aalten DM, Bywater R, Findlay JB, Hendlich M, Hooft RW, Vriend G (1996) PRODRG, a program for generating molecular topologies and unique molecular descriptors from coordinates of small molecules. *J Comput Aided Mol Des* **10**: 255–262
- Wang C, Wang K, Wang W, Cui Y, Fan Z (2002) Compromised ATP binding as a mechanism of phosphoinositide modulation of ATP-sensitive K⁺ channels. *FEBS Lett* **532**: 177–182
- Yorifuji T, Nagashima K, Kurokawa K, Kawai M, Oishi M, Akazawa Y, Hosokawa M, Yamada Y, Inagaki N, Nakahata T (2005) The C42R mutation in the Kir6.2 (KCNJ11) gene as a cause of transient neonatal diabetes, childhood diabetes, or later-onset, apparently type 2 diabetes mellitus. *J Clin Endocrinol Metab* **90**: 3174–3178